Preprints (www.preprints.org) | NOT PEER-REVIEWED | Posted: 31 August 2021 doi:10.20944/preprints202108.0554.v1

Article

Biomass Burning and Gas Flares create the extreme West African Aerosol Plume which perturbs the Hadley Circulation and thereby changes Europe's winter climate

Keith A. Potts[1]

1. Kyna Keju Pty Ltd;
* Correspondence: Keith.Potts@bigpond.com;

Abstract: Europe's winter climate has experienced three significant changes recently: increased UK flooding; Iberian drought; and warmer temperatures north of the Alps. The literature links all three to a persistent, significant increase in sea level pressure over the Mediterranean and Iberia which changes the atmospheric circulation system by: forcing cold fronts north away from Iberia; and creating a south westerly flow around the high-pressure region bringing warmer, moist air from the subtropical Atlantic to Europe which increases UK precipitation and European temperatures. Here I show, using modelled, reanalysis and measured data, that: the extreme, anthropogenic, West African aerosol Plume (WAP) which exists from late December to early April perturbs the northern, regional Hadley Circulation creating the high-pressure region; and that the WAP has only existed in its extreme form in recent decades as the major sources of the aerosols: biomass burning; and gas flaring have both increased significantly since 1950 due to: a four-fold increase in population (United Nations); and gas flaring rising from zero to 7.4 billion m3/annum (Global Gas Flaring Reduction Partnership). I also suggest that the WAP can be eliminated and Europe's winter climate returned to its natural state after the crucial first step of recognising the cause of the changes is taken.

Keywords: Biomass burning; Anthropogenic aerosols; West Africa; United Kingdom Floods; Iberian Drought; European winter temperatures; Last Millennium Ensemble; NASA MERRA-2;

© 2021 by the author(s). Distributed under a Creative Commons CC BY license.

Preprints (www.preprints.org) | NOT PEER-REVIEWED | Posted: 31 August 2021 doi:10.20944/preprints202108.0554.v1

INTRODUCTION

The extreme West African aerosol Plume (WAP) is one of eight continental scale aerosol plumes (Appendix A). It perturbs the northern Hadley circulation in winter creating anomalous high pressure over Southern Europe, the Mediterranean Sea, Iberia and the Eastern Atlantic (SEMIEA) which creates floods in the United Kingdom (UK), drought in Iberia and warmer temperatures north of the Alps.

1.1 Floods in the United Kingdom

The UK has experienced significant floods in winter and early spring in recent decades with 1998, 2000, 2001, 2002, 2005, 2009, 2010, 2012, 2014, 2015, 2019 and 2020 noted as significant rainfall/flood events on the UK Met. Office website demonstrating a return frequency of about 2 years. In 2020 and 2021 storms Ciara, Dennis, Bella and Christoph unleashed more UK floods with Dennis causing an estimated five fatalities in the UK (Mirror https://www.mirror.co.uk/news/uk-news/fears-missing-woman-87-sixth-21530531) and the Association of British Insurers estimating the damage at £360 million (https://www.abi.org.uk/news/news-articles/2020/03/insurance-pay-outs-to-help-customers-recover-from-storms-ciara-and-dennis-set-to-top-360-million/). Determining the cause of such events and why they are of such severity in recent decades is therefore crucial socially, economically and scientifically to enable mitigation action to start.

The literature includes:

- From a 558 year paleorecord of floods derived from Lake Bassenthwaite sediment "the cluster of devastating floods from 1990 to present is without precedent" [1] . This time period coincides with the WAP reaching average aerosol optical depth (AOD) levels from January to March (JFM) consistently above 0.5 in the MERRA-2 [2] data.
- In winter in 2013-14 a rapid succession of Atlantic low pressure systems crossed the UK with large increases in rainfall in the south of England and much of Scotland [3] noting "The role of anthropogenic aerosol effects requires further work, especially on tropical atmospheric circulation and hence rainfall".
- A regional climate model investigation into the effects of anthropogenic emissions on the winter climate of the UK [4] only refers to "sulphate aerosol precursors" and it cannot therefore have included the effects of the WAP which is predominantly carbonaceous (Appendix B). However, the paper noted "More studies of this nature are needed if loss and damage from anthropogenic climate change are to be quantified objectively and future assessments of the impacts of climate change are to progress from attributing them simply to changes in climate which are not themselves explained, to attributing them specifically to human influence.".
- Atmospheric rivers flowing from the subtropical Atlantic preceded the ten largest winter flood events in British river

Preprints (www.preprints.org) | NOT PEER-REVIEWED | Posted: 31 August 2021 doi:10.20944/preprints202108.0554.v1

basins and the SW-NE tilt in the large-scale atmospheric flow is crucial [5]. Figure 2(b) in this paper shows high pressure over SEMIEA.

1.2 *Drought in Spain*

A significant driver of the 2004/05 hydrological year drought in Iberia was "an impressive northward displacement of cyclone trajectories in the North Atlantic sector in winter months resulting in an almost complete absence of cyclones crossing Iberia and western Europe." [6] and "The results … show the (North Atlantic Oscillation) NAO and (East Atlantic) EA indexes …incapable to detect the low precipitation totals in March.".

An increase in the number of anti-cyclonic (higher than average pressure) days in winter from 1950 to 2000 which results in lower rainfall in NE Spain was found in an investigation of the relationship between the occurrence of drought in NE Spain and atmospheric circulation [7].

Preprints (www.preprints.org) | NOT PEER-REVIEWED | Posted: 31 August 2021 doi:10.20944/preprints202108.0554.v1

1.3 *Higher Winter Temperatures in Northern Europe*

The Intergovernmental Panel on Climate Change (IPCC) identified Europe as one of the fastest warming regions and Assessment Report 4 (AR4) discussing changes since 1979 stated: "Warming in this period was strongest over western North America, northern Europe and China in winter". AR5 states "Regardless of whether the statistics of flow regimes themselves have changed, observed temperatures in recent years in Europe are distinctly warmer than would be expected for analogous atmospheric flow regimes in the past, affecting both warm and cold extremes citing [8] [9].

The European winter of 2006-07 was exceptionally warm and the temperatures experienced during autumn 2006 and winter 2007 are likely to have been the warmest in 500 years [10]. The winter temperature rise in Europe is dominated by circulation changes that bring mild maritime air into Europe north of the Alps and climate modelling fails to replicate these circulation changes – specifically the higher pressure over the SEMIEA [11] [12]. The SEMIEA high-pressure anomaly advects warm air from the central Atlantic to northern Europe resulting in anomalously high temperatures [11].

These papers demonstrate that the climate modelling which was reviewed did not include the forcing agent which caused the rise in pressure over the SEMIEA which I show to be the carbonaceous WAP.

1.4 *Pressure over the Mediterranean and the Iberian Peninsula*

All three changes outlined above are linked to increased sea level pressure over the SEMIEA in the winter months. "Changes in atmospheric circulation are important for local climate change because they could lead to greater or smaller changes in climate in a particular region than elsewhere. It is likely that human influence has altered sea level pressure patterns globally." (AR5). This paper demonstrates this exactly, the anthropogenic WAP creates the increase in pressure over the SEMIEA which drives the changes in the winter climate of Europe.

Trends in sea-level pressure in Europe are shown in Figure 7 of [11] which shows a significant increase in pressure in the SEMIEA from 1950–2007. Comparisons of observed changes and climate model simulations are also included and for two models the observed trend in pressure is a factor of four larger than the modelled trend whilst another two models show smaller trends and two no trends at all. In the ESSENCE ensemble only tropospheric sulphate aerosols are included in the historic data [13] and the ensemble cannot therefore have modelled the WAP correctly as it is predominantly carbonaceous

1.5 *The Anthropogenic West African Aerosol Plume*

Figure 1 shows the areas used:

1. AOD (WAP Area): 0° 10°N and 0° 10°E
2. Surface Temperature (WAP (ST)): 6° 12°N and 5°W 5°E

Preprints (www.preprints.org) | NOT PEER-REVIEWED | Posted: 31 August 2021 doi:10.20944/preprints202108.0554.v1

3.	Omega West Africa (W. Africa): and 0° 10E°		10°	15°N	
4.	Pressure (SEMIEA): 30°W 15°E	30°	45°N	and	
5.	Rainfall Southern Europe (MIEA): and 20°W 10°E		35°	43°N	
6.	Rainfall Northern Europe (UK): and 10°W 10°E		50°	60°N	
7.	Temperature (Northern Europe): and 15°W 30°E		45°	60°N	

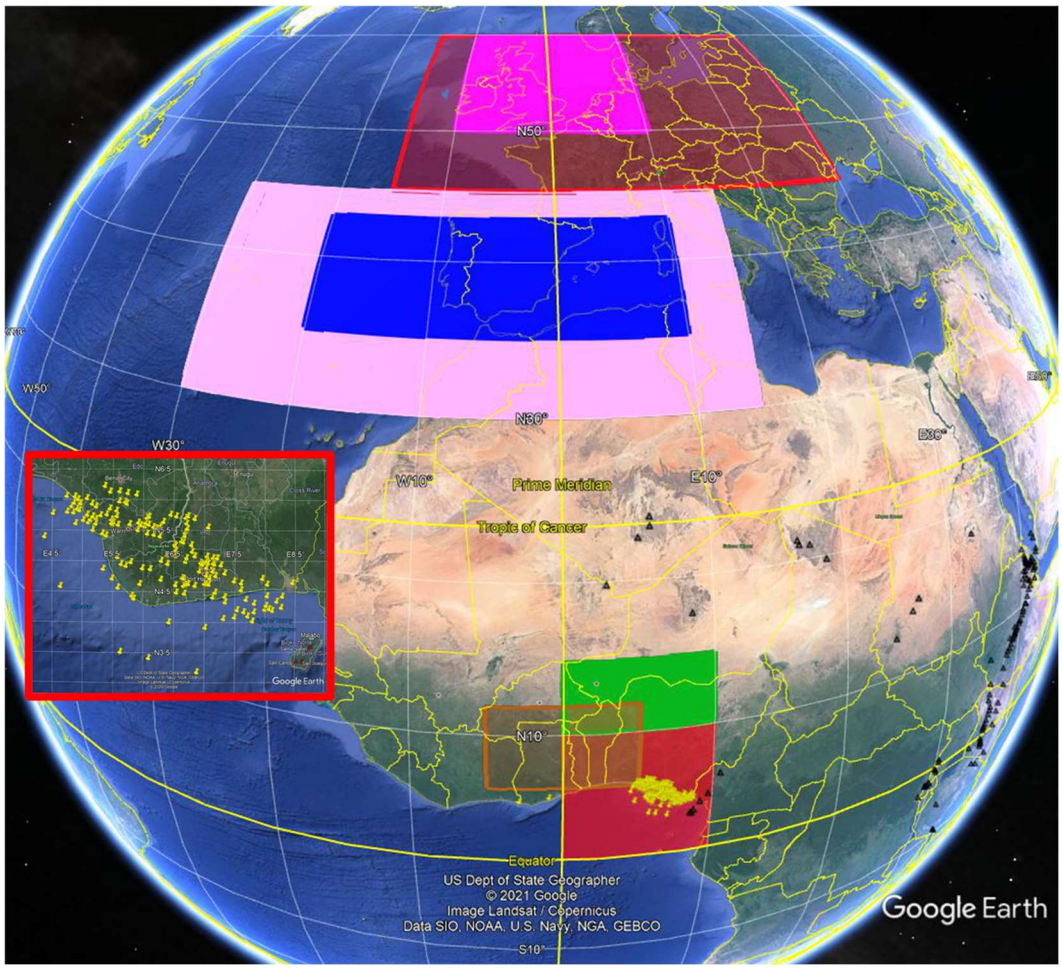

Figure 1. Google Earth image showing: areas used; locations of Nigerian gas flares (National Oceanic and Atmospheric Administration (NOAA) and the Global Gas Flaring Reduction Partnership (GGFRP)) in yellow; and African volcanoes (Global Volcanism Program) in black. Inset southern Nigerian gas flares.

The WAP's location, West Africa, and season means it will perturb the European regional Hadley Circulation in winter. Appendix B describes the main aerosol sources and shows they are entirely anthropogenic.

Preprints (www.preprints.org) | NOT PEER-REVIEWED | Posted: 31 August 2021 doi:10.20944/preprints202108.0554.v1

The WAP is one of eight great aerosol plumes (Appendix A) which occur annually. It can be identified on the monthly mean 0.55 micron AOD data from MODIS [15] on the NASA Terra satellite distributed via NASA Giovanni. The uncertainty in the AOD measured by this satellite is "$\Delta\tau=\pm0.05 \pm0.15\tau$ over land" and the AOD retrievals can be used in monitoring the aerosol radiative forcing of the global climate [16] [17].

The monthly average WAP Area AOD and the annual AOD cycle are shown in Figure 2 to demonstrate the peak aerosol emission season is January to March (JFM), the end of the dry season. I focus on JFM because the WAP will have its greatest effect at this time. Figure 3 shows the MERRA-2 reanalysis JFM AOD data for the WAP Area which varies significantly.

Preprints (www.preprints.org) | NOT PEER-REVIEWED | Posted: 31 August 2021 doi:10.20944/preprints202108.0554.v1

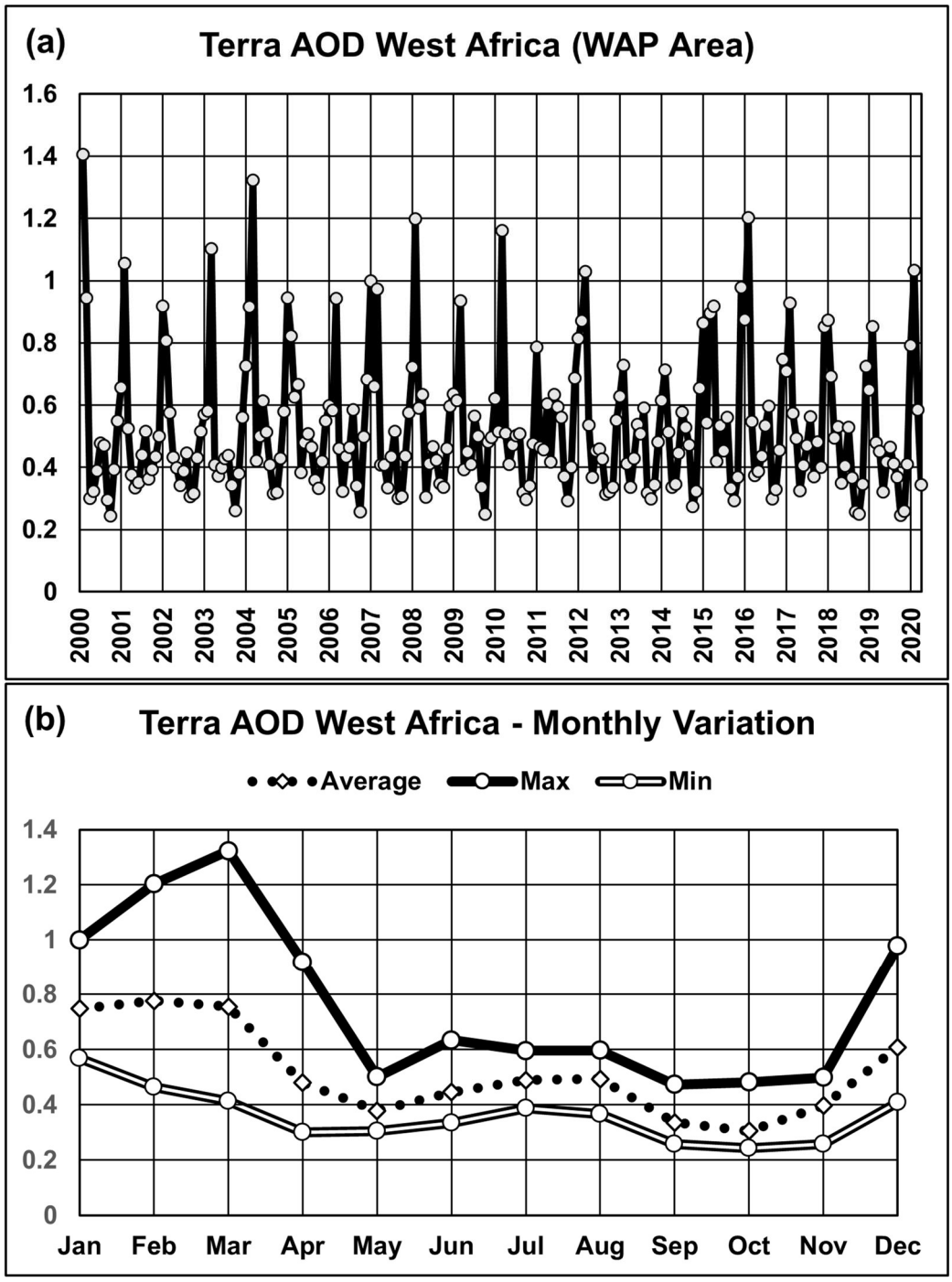

Figure 2. (a) Terra Monthly AOD WAP Area; (b) Average, Max and Min Annual cycle.

Preprints (www.preprints.org) | NOT PEER-REVIEWED | Posted: 31 August 2021 doi:10.20944/preprints202108.0554.v1

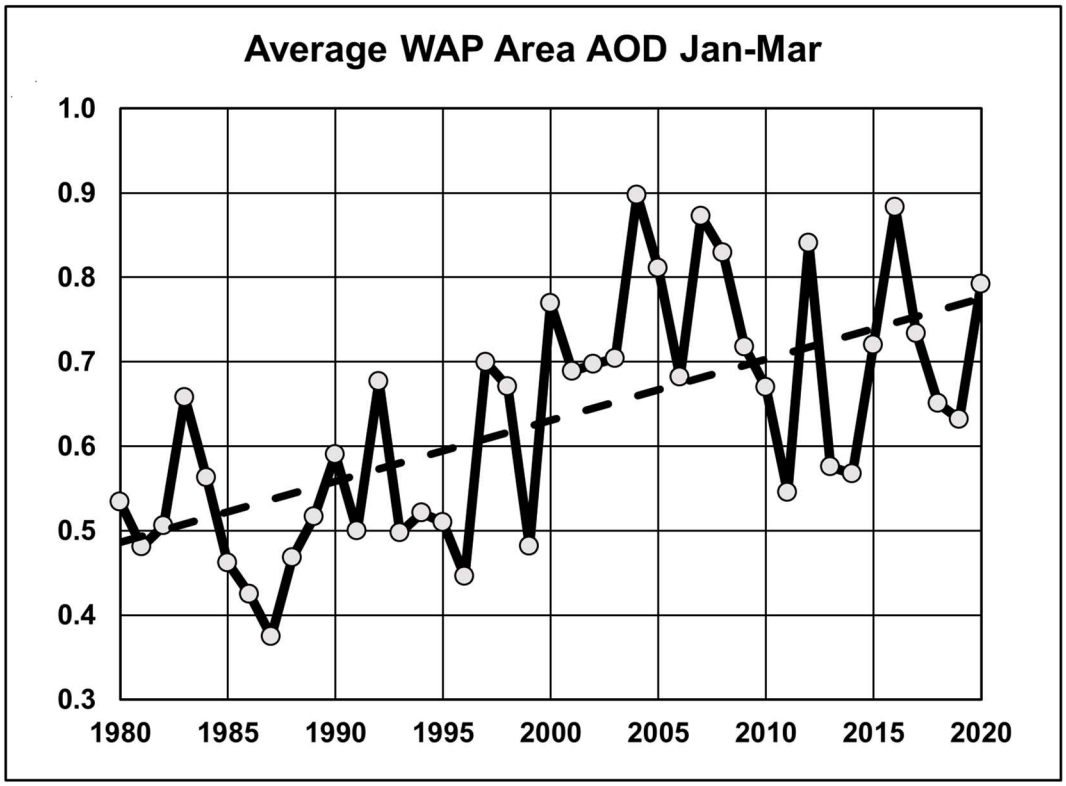

Figure 3. MERRA-2 JFM AOD WAP Area.

The maximum AOD for the WAP was 1.41 (Feb 2000) and the trend line of the MERRA-2 AOD in JFM in the WAP Area increased from 0.48 in 1980 to 0.77 in 2020 a 60% increase. From 1980 to 2004, a major biomass burning event year, the increase in AOD in March was from 0.37 to 1.10 a three-fold increase.

Preprints (www.preprints.org) | NOT PEER-REVIEWED | Posted: 31 August 2021 doi:10.20944/preprints202108.0554.v1

Figure 4 shows the geographic extent of the JFM 2004 extreme apparition of the WAP and shows the plume's origin to be in southern Nigeria.

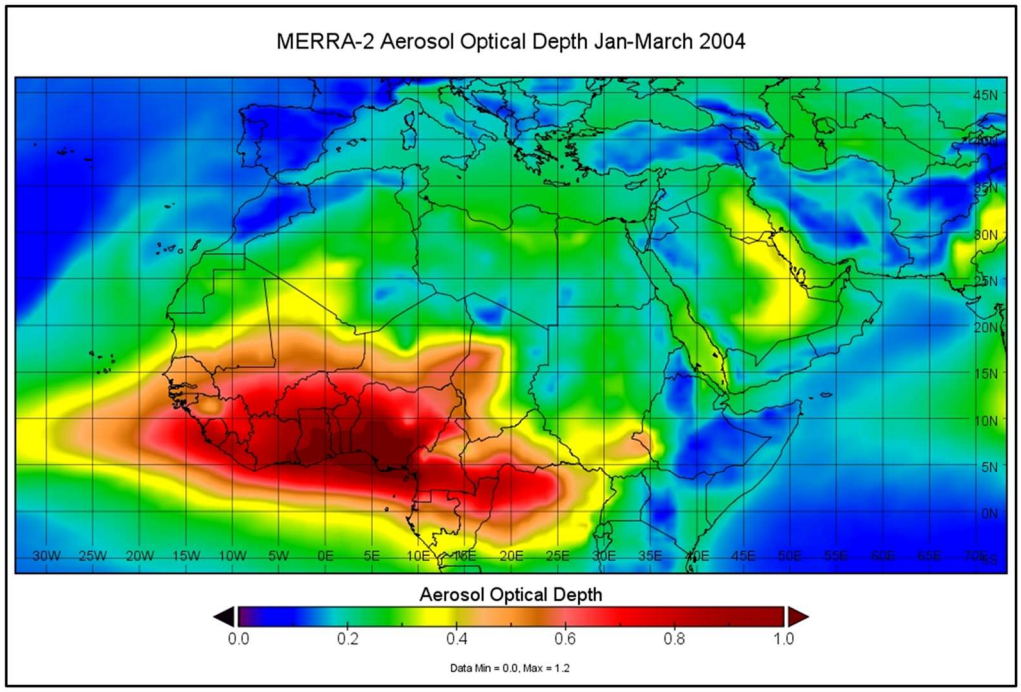

Figure 4. MERRA-2 JFM average AOD 2004.

The AOD retrievals from the NASA Terra and Aqua satellites and ground-based photometers were found to correlate well, over 0.90, at Ilorin in Nigeria [18]. Figure 2 in that paper clearly shows the seasonal variation in the AOD levels with many days showing AOD levels over 1.00 in JFM from 2005 to 2009.

WAP History: Figure 3 shows a significant trend in the AOD of the WAP from 1980 to 2020 and the WAP AOD would have been significantly lower in 1950 than in 1980 as:

- The population of West Africa increased from 71 million in 1950 to 188 million in 1980 (United Nations World population data for West Africa) which implies less biomass burning from agriculture and land clearing in 1950 and therefore a lower aerosol burden from these sources; and
- Oil production started in Nigeria in 1958 (Nigerian National Petroleum Corporation in "History of the Nigerian Petroleum Industry" at https://www.nnpcgroup.com/NNPC-Business/Business-Information/Pages/Industry-History.aspx) and there were therefore no aerosol producing gas flares in Nigeria in 1950.

The estimated WAP AOD in 1950 (JFM) is 0.09 on the basis of pro rata population and oil production changes and confirmed by projecting the trend of the lower AOD levels in the MERRA-2 data

Preprints (www.preprints.org) | NOT PEER-REVIEWED | Posted: 31 August 2021 doi:10.20944/preprints202108.0554.v1

(1987, 1996) back to 1950 (0.08). This implies the effects of the extreme WAP are very recent and that the anthropogenic WAP probably did not exist in its present extreme state in JFM before the early 1970's as oil production did not reach one million barrels per day until 1970 (BP 2019).

Personal Note: I lived in southern Nigeria between 1968 and 1972 and saw no extreme levels of smoke in the atmosphere in those years.

1.6 Surface Radiative Forcing (SF) by Aerosols

Aerosol SF is significant: 10% to 30% reduction [19]; -150 W/m^2 [20]; and -286(W/ m^2)/(unit AOD) [21].

Figure 5 shows the MERRA-2 surface radiation and AOD averaged across the WAP Area longitudes with 1987, the lowest WAP Area JFM AOD subtracted from 2004, the highest, to show the 2004 anomaly. The series correlate at -0.98 (significance << 0.01) and it is clear that the increase in AOD in 2004 has caused a maximum SF of -37 W/m^2 and an average from 6.75ºS to 12.25ºN of -21.2 W/m^2.

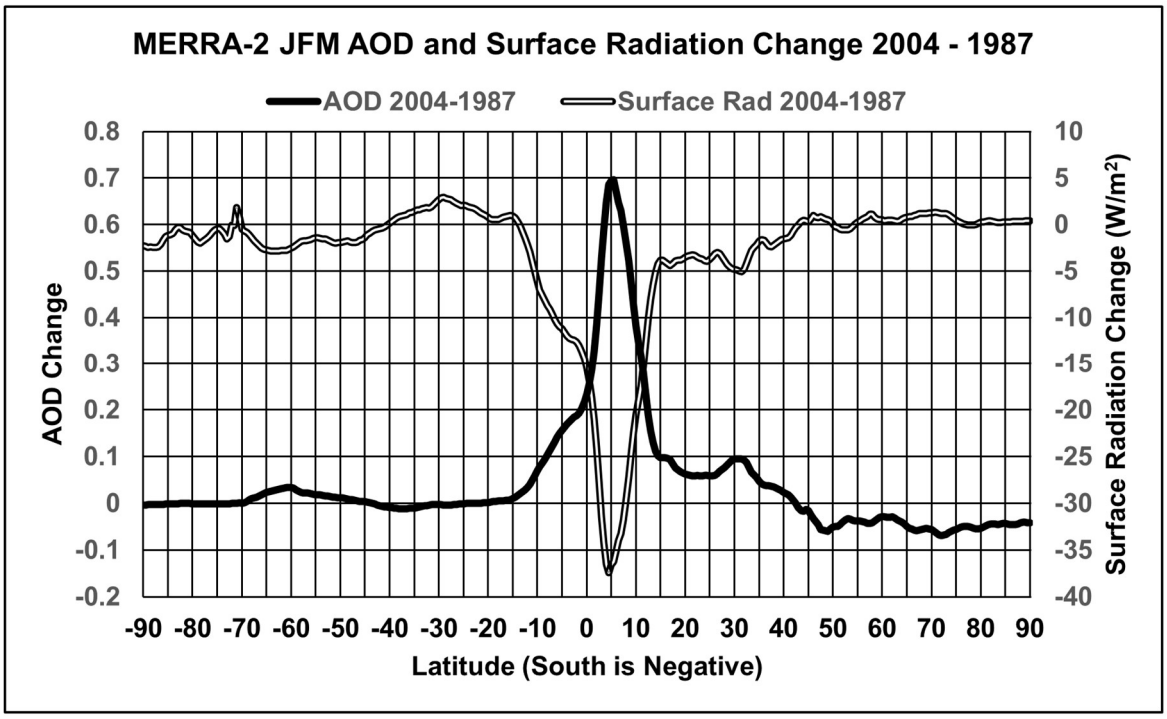

Figure 5. MERRA-2 JFM clear sky surface solar radiation and WAP AOD averaged across the WAP Area longitudes. 1987 data (lowest AOD year) subtracted from 2004 (highest AOD Year).

This 21.2 W/m^2 reduction implies that across the WAP Area alone 1,104 by 1,109 km the total reduction in surface radiation is 2.6 x 10^{13} W and would be significantly greater when calculated across the entire plume (Figure 4). This is a dramatically large change in the surface radiation budget, well capable of modifying the atmospheric circulation. The northern Hadley Circulation convection will move

Preprints (www.preprints.org) | NOT PEER-REVIEWED | Posted: 31 August 2021 doi:10.20944/preprints202108.0554.v1

north of the WAP which forces the entire circulation north and creates the anomalous, persistent, high pressure over the SEMIEA as a direct consequence of the WAP.

Note: The 1987 WAP JFM AOD was 0.38 which is significantly higher than the 1950 estimate (0.09) and the SF of the WAP in 2004 cf. 1950 would be even greater.

Appendix C discusses aerosols and climate.

METHOD

Appendix D shows the data sources.

Data was detrended using PAST3 [22].

1.7 Last Millennium Ensemble

LME [23] data analysed is: atmosphere, post processed monthly averages consisting of seven simulations (Table 1 [23]) plus "850" which were repeated in multiple runs. Aerosol Optical Depth (AOD) (AODVIS), surface pressure (PSL), surface temperature (TS), precipitation (PRECL) and vertical pressure velocity (omega) data from these simulations(run) was used: 850(003); Green House Gas(003); Orbital(003) Land Use(003); Solar(005); Volcanic(005); Ozone & Aerosols(002); All(013). Each simulation(run) was processed separately to give: JFM average data for each parameter for the required areas as a 1,156 element time series; and annual AOD and omega data.

1.8 MERRA-2 Data

MERRA-2 data is an independent dataset used to:

1. Confirm the LME analysis;
2. Show the geographical extent of the WAP effects in Appendix E.

1.9 Terra and NCEP/NCAR Reanalysis

Terra and NCEP/NCAR [24] data provide another independent confirmation of the WAP effects. Terra data derives from the MODIS sensor and the NCEP/NCAR data is used in the analysis of the anomalous high pressure over SEMIEA [11].

RESULTS

Results are presented as scatter plots showing:

1. Eight LME simulations/runs combined, a total of 8,248 data points;
2. LME(S) all LME data segmented in bins from AOD less than 0.45 in steps of 0.05 to over 0.90;
3. MERRA-2 (1980-2020);
4. Terra-NCEP/NCAR (TN) (2000-2020);

with the trend line, trend line equation and R^2 for each dataset and Table 1 showing:

1. The JFM time series correlations from the graphs;
2. Trend per unit AOD increase in the WAP from the graphs;
3. Change over the AOD range in that dataset;
4. Change from 1950 AOD to the maximum AOD level;
5. Percentage rainfall changes from 1950 AOD to the dataset maximum.

Preprints (www.preprints.org) | NOT PEER-REVIEWED | Posted: 31 August 2021 doi:10.20944/preprints202108.0554.v1

Table 1. Correlations, trend and changes from: minimum to maximum JFM AOD; and from the estimated 1950 JFM AOD to maximum JFM AOD for the parameters shown in the LME, MERRA-2 and Terra-NCEP/NCAR datasets. Significance is <0.10 Underline, *<0.05 Italic*, ***<0.02 Bold Italic,*** **<0.01 Bold.**

A	Surface Temp W Africa	LME	LME(S)	MERRA-2	Terra NCEP/NCAR
1	R	**-0.66**	**-0.99**	-0.22	-0.15
2	R^2	**0.43**	**0.99**	0.05	0.02
3	Trend/unit AOD (ºK)	-3.06	-3.10	-1.63	-0.45
4	Change over AOD range (ºK)	-3.15	-1.52	-0.66	-0.23
5	1950 AOD to max AOD (ºK)	-3.63	-2.64	-1.27	-0.45
B	**Omega W Africa**				
1	R	**0.71**	**0.99**	**0.54**	*0.48*
2	R^2	**0.50**	**0.99**	**0.29**	*0.23*
3	Trend/unit AOD (Pa/s)	0.05	0.05	0.08	0.07
4	Change over AOD range (Pa/s)	0.05	0.03	0.03	0.04
5	1950 AOD to max AOD (Pa/s)	0.06	0.04	0.06	0.07
C	**MSLP SEMIEA**				
1	R	**0.75**	**0.99**	0.29	**0.60**
2	R^2	**0.56**	**0.99**	0.08	**0.36**
3	Trend/unit AOD (hPa)	13.2	13.15	5.5	15.0
4	Change over AOD range (hPa)	13.6	7.24	2.9	7.5
5	1950 AOD to max AOD (hPa)	15.6	11.59	4.4	14.9
D	**Rainfall MIEA**				
1	R	**-0.64**	**0.99**	**-0.42**	***-0.54***
2	R^2	**0.41**	**0.98**	**0.18**	***0.29***
3	Trend/unit AOD (mm)	-189	-188	-186	-243
4	Change over AOD range (mm)	-194	-103	-75	-122
5	1950 AOD to max AOD (mm)	-224	-166	-145	-241
6	Percentage change from 1950	-97%	-71.8%	-58%	-75%
E	**Rainfall UK**				
1	R	**0.42**	**0.98**	0.10	*0.47*
2	R^2	**0.18**	**0.96**	0.01	*0.22*
3	Trend/unit AOD (mm)	236	236	24	157
4	Change over AOD range (mm)	243	127	13	79
5	1950 AOD to max AOD (mm)	280	208	19	156
6	Percentage change from 1950	72%	54%	8%	197%
F	**Temperature Europe**				
1	R	**0.45**	**0.99**	*0.33*	0.29
2	R^2	**0.20**	**0.98**	*0.11*	0.08
3	Trend/unit AOD (ºK)	2.45	2.43	3.68	2.76
4	Change over AOD range (ºK)	2.52	1.3	1.48	1.38
5	1950 AOD to max AOD (ºK)	2.90	2.14	2.87	2.73

Note that:

- Some LME correlations show significance levels much less than 0.01 due to the correlation magnitude and time series length.

Preprints (www.preprints.org) | NOT PEER-REVIEWED | Posted: 31 August 2021 doi:10.20944/preprints202108.0554.v1

- The AOD range in the datasets is Terra 0.6 to 1.1, MERRA-2 0.4 to 0.9 and the LME 0.3 to 1.1. The LME and MERRA-2 AOD ranges are similar whilst the Terra dataset shows a higher low value than the others as the WAP was well established for the entire dataset and was not for the LME and MERRA-2 data (Figures 2 and 3).

Appendix E shows comparison JFM images for each parameter analysed created by subtracting the 1987 data (low WAP AOD) from 2004 (high WAP AOD) using NASA Panoply and the NCEP/NCAR website.

1.10 The WAP Forms

The intense WAP forms in late December and disperses in April (Figure 2). Figure A8 shows an increase in JFM AOD of over 0.6 across half the WAP Area.

1.11 The WAP absorbs Solar Radiation and Heats the Atmosphere

Figure A9 shows the MERRA-2 air temperature comparison averaged across the WAP Area longitudes from 20°S to 40°N. In 2004 the air temperature within the plume at 700hPa to 850hPa is ~1º K higher which matches the estimated aerosol height from CALIPSO data [25] on 1 January 2016 (high WAP AOD) showing elevated aerosol levels at altitudes from 1.0 to 5.0 km.

1.12 The WAP Reduces the WAP Land Area Surface Temperature

The LME data in Table 1 (A)(1-2) shows a statistically significant connection between the WAP AOD and surface temperature. Whilst not showing statistical significance the MERRA-2 and Terra-NCEP/NCAR trend data in Table 1 and Figure 6 also show reducing surface temperature with increasing AOD. Figure A10 shows a reduction of over 2º K.

Preprints (www.preprints.org) | NOT PEER-REVIEWED | Posted: 31 August 2021 doi:10.20944/preprints202108.0554.v1

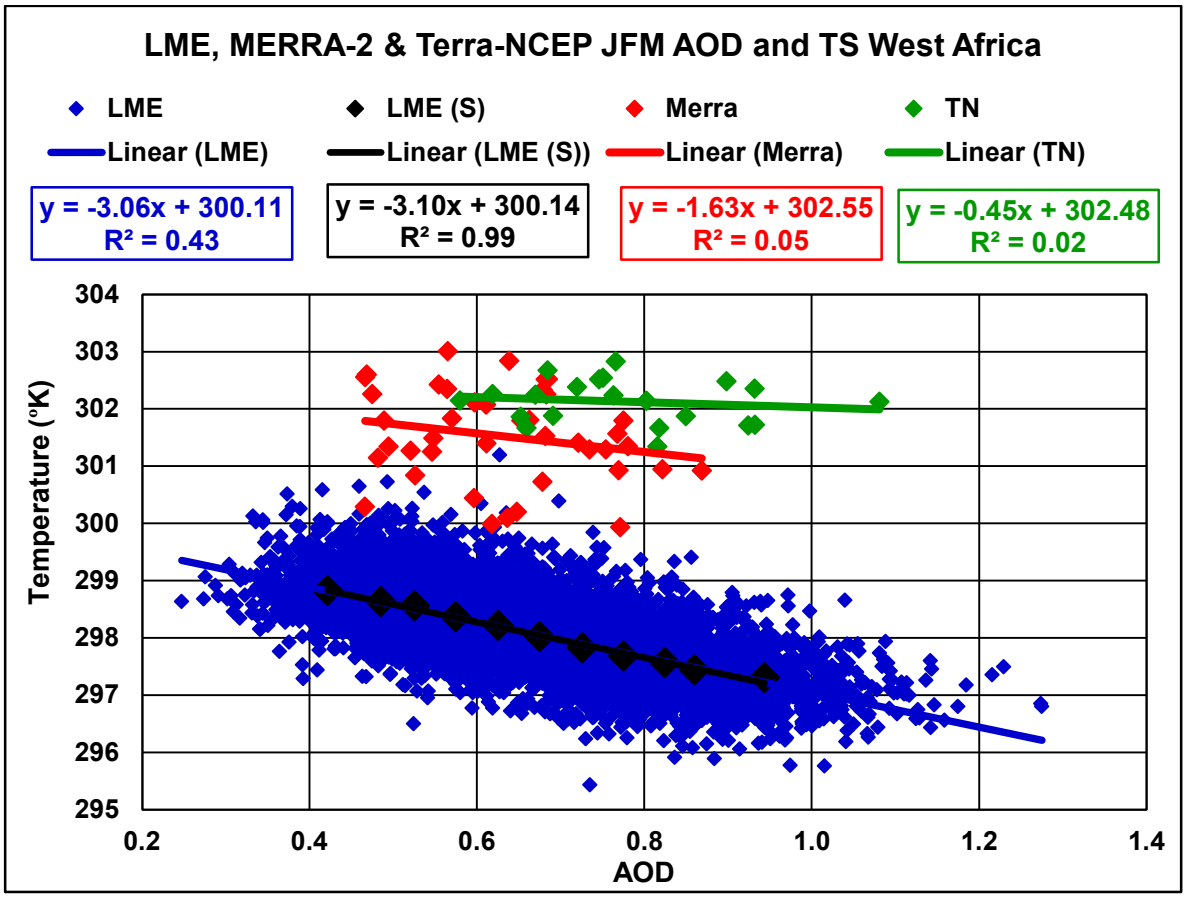

Figure 6. LME, MERRA-2 and Terra-NCEP/NCAR JFM Surface Temperature West Africa and WAP Area AOD.

1.13 The WAP Reduces Convection in West Africa

The LME, MERRA-2 and Terra-NCEP/NCAR data in Table 1 (B)(1-2) all show a statistically significant connection between the WAP AOD and omega at 820 hPa in West Africa. All datasets at (B)(3-5) and Figure 7 show positive increases in omega (reductions in convection) as the WAP AOD increases and:

1. Both the MERRA-2 and Terra-NCEP/NCAR data show higher trends per unit AOD than the LME;
2. The trend line in the LME data in Figure 7 shows that, on average, when the WAP AOD rises over 0.8 omega becomes positive implying that convection reverses at this level in the model; and
3. Figure A11 shows a 0.03 Pa/s increase in omega

Note: rising air creates negative omega as it moves from higher to lower pressure. Reducing convection creates a positive change in omega and as aerosols reduce convection the correlations of omega and AOD are positive.

Preprints (www.preprints.org) | NOT PEER-REVIEWED | Posted: 31 August 2021 doi:10.20944/preprints202108.0554.v1

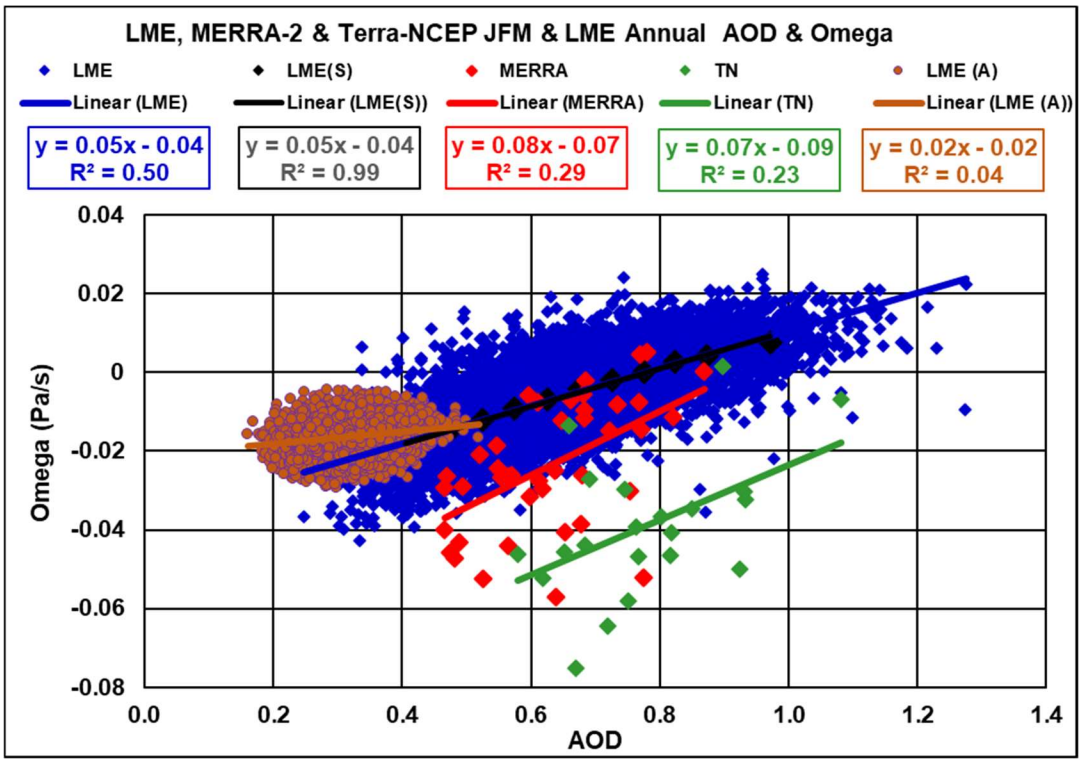

Figure 7. LME, MERRA-2 and Terra-NCEP/NCAR JFM Omega and WAP Area AOD and LME Annual Data.

Figure 7 includes LME annual data which demonstrates how averaging the effects of aerosol plumes annually when the "extreme" plume only exists for a few months completely destroys the significant seasonal effects of the plume. The annually averaged data shows: R^2 values an order of magnitude less than the JFM values; omega only rising from -0.017 to -0.015; and no reversal of convection seen in the JFM data as it is masked by the averaging. This conclusively demonstrates that aerosols must be analysed at spatial and temporal resolutions which can correctly model the plume. The effects of carbonaceous aerosols on surface radiation, convection and atmospheric circulation have been extensively described in the literature (Appendix C). The WAP absorbs solar radiation: warming the upper atmosphere; and cooling the surface and lower atmosphere. This alters the vertical temperature profile of the atmosphere with warmer air above cooler (relative to the temperatures without the plume) stabilising the atmosphere and reducing convection. This well understood process is confirmed in the WAP Area with the correlation of omega and AOD in Table 1(B)(1-2) and Figure 7.

1.14 *The WAP Perturbs the Hadley Circulation:*

The Hadley Cells are thermally driven [26] [27] [28] and reduced surface solar radiation therefore reduces convection in the WAP Area which perturbs the regional Hadley Cell and this can be clearly seen in Figure A11 where the rising limb of the northern Hadley Cell has been altered in 2004 cf. 1987 and the region showing the greatest

Preprints (www.preprints.org) | NOT PEER-REVIEWED | Posted: 31 August 2021 doi:10.20944/preprints202108.0554.v1

increase in convection is between 25° and 35° north which is north of the WAP (Figure 4).

1.15 *The Crucial Step – The WAP Increases Surface Pressure in the SEMIEA*

The LME, MERRA-2 and Terra-NCEP/NCAR data in Table 1 (C)(1-2) all show a statistically significant connection between the WAP AOD and PSL in the SEMIEA. All datasets at (C)(3-5) and Figure 8 show increases in PSL as the WAP AOD level increases and note that: The Terra-NCEP/NCAR data shows a higher trend than the LME in Figure 8; and Figure A12 shows a 3 to 5 hPa increase in PSL 2004-1987 which is similar to the trend in [11].

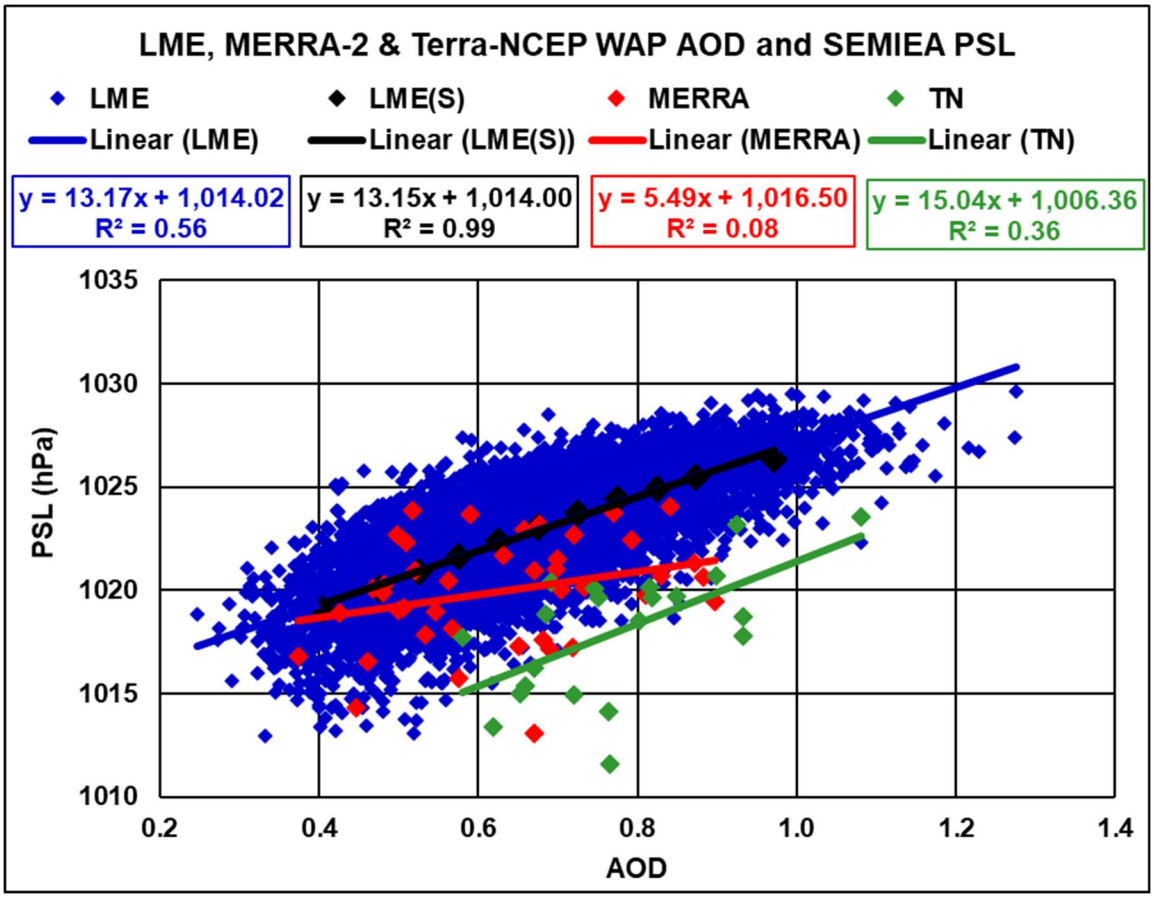

Figure 8. LME, MERRA-2 and Terra-NCEP/NCAR JFM Surface Pressure and WAP Area AOD.

The estimated LME and Terra-NCEP/NCAR change from 1950 to the post 2000 average high AOD in Table 1 (C)(5) is greater than the changes shown in Figure 7 of [11] from 1950 to 2007 which the modelling cited in the paper does not replicate.

Figure A11 shows that a major increase in omega occurs between 35ºN and 45ºN which leads to higher SEMIEA pressure.

This is the crucial step in the changes induced by the WAP and is the only change remote from West Africa directly forced by the WAP

Preprints (www.preprints.org) | NOT PEER-REVIEWED | Posted: 31 August 2021 doi:10.20944/preprints202108.0554.v1

by the perturbation of the Hadley Circulation with all other changes, UK flooding, Iberian drought and higher European winter temperatures being secondary effects which are driven by this anomalous and persistent region of increased pressure.

1.16 The WAP Reduces Precipitation in the MIEA

The LME, MERRA-2 and Terra-NCEP/NCAR data in Table 1 (D)(1-2) all show a statistically significant connection between the WAP AOD and PRECL in the MIEA. All datasets at (D)(3-6) and Figure 9 show reductions in PRECL as the WAP AOD level increases and note that: The Terra-NCEP/NCAR data shows a larger negative trend per unit AOD change than the LME and the average percentage reduction in rainfall across the four datasets in Table 1(D)(6) is 75% which is similar to the reported reduction of 60% [6]. Figure A13 shows up to 60mm reduction in MIEA JFM PRECL.

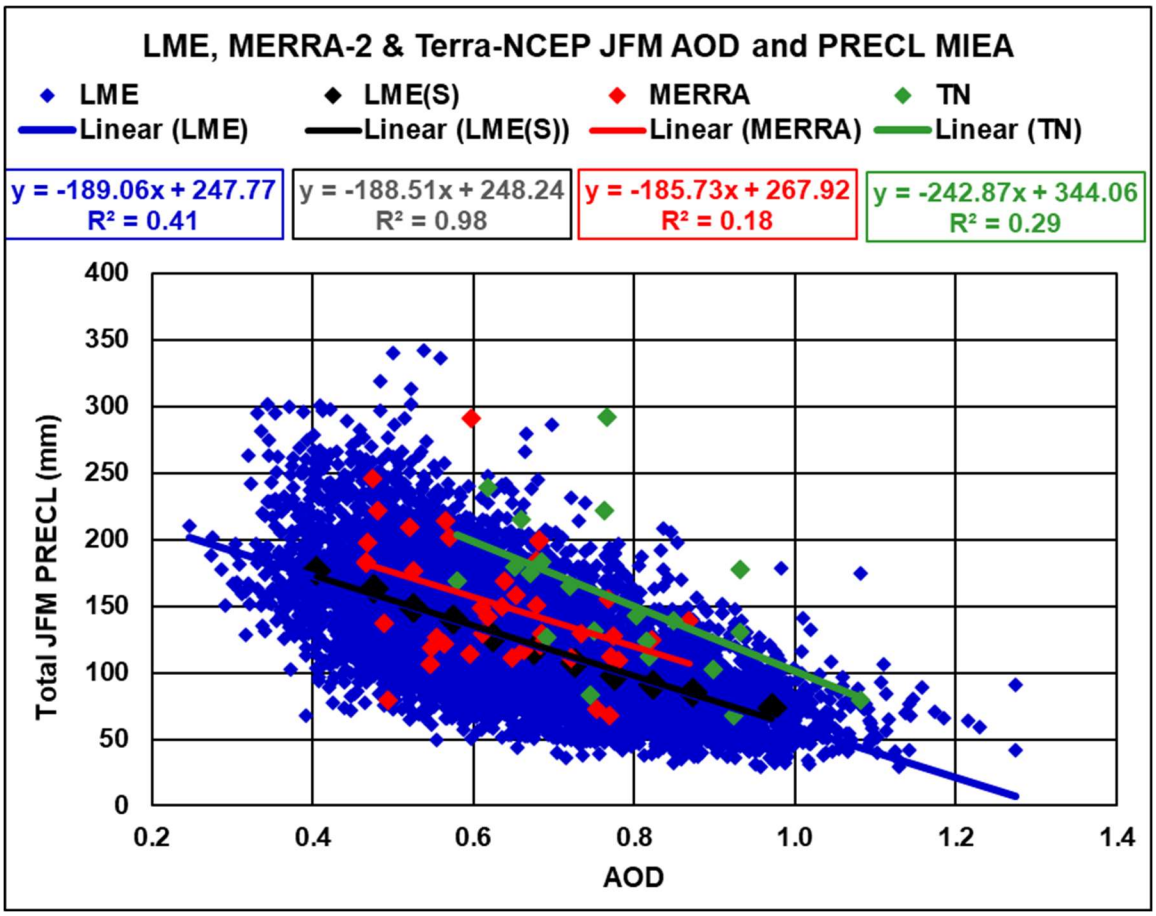

Figure 9. LME, MERRA-2 and Terra-NCEP/NCAR JFM MIEA Precipitation and WAP Area AOD.

1.17 The WAP Advects Warm, Moist Air into Northern Europe

With high pressure established over the SEMIEA (Figure A12) the natural wind flows are perturbed. Figure A14 shows a strong flow from the Atlantic Ocean east of the USA travelling north east into the

Preprints (www.preprints.org) | NOT PEER-REVIEWED | Posted: 31 August 2021 doi:10.20944/preprints202108.0554.v1

UK and northern Europe which constitutes an atmospheric river carrying significant moisture from the warm ocean to the UK [5] [29] and for an early overview [30] [31].

1.18 The WAP Increases Precipitation in the UK

The LME and Terra-NCEP/NCAR data in Table 1 (E)(1-2) show statistically significant connections between the WAP AOD and PRECL in the UK. All datasets at (E)(3-6) and Figure 10 show increasing UK PRECL as the WAP AOD level increases and note that the Terra-NCEP/NCAR data shows the largest percentage increase at (E)(6) being more than double the LME increase. Figure A13 shows an increase of up to 60 mm in JFM PRECL.

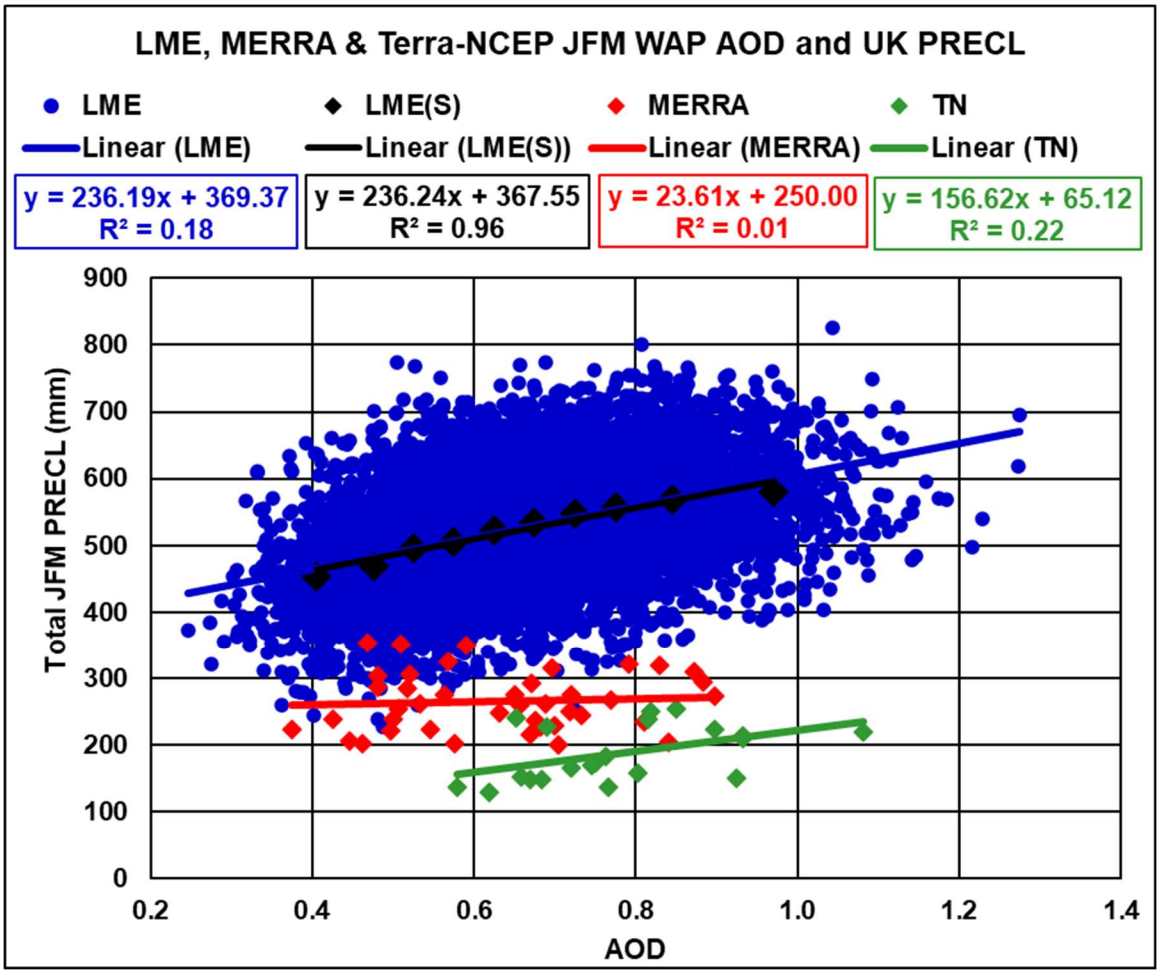

Figure 10. LME, MERRA-2 and Terra-NCEP/NCAR JFM UK Precipitation and WAP Area AOD.

The average increase of 165 mm in Table 1 (E)(5) from 1950 to the high AOD is of similar, but higher, magnitude to the change in the JFM rainfall in Dunstaffnage in western Scotland recorded by the UK Met Office at https://www.metoffice.gov.uk/pub/data/weather/uk/climate/stationda

Preprints (www.preprints.org) | NOT PEER-REVIEWED | Posted: 31 August 2021 doi:10.20944/preprints202108.0554.v1

ta/dunstaffnagedata.txt from 411mm (pre 1991) to 515 mm (post 1990) at + 104mm.

Also note that atmospheric rivers from the subtropical Atlantic to the UK only occur because low pressure systems moving eastwards across the Atlantic meet the persistent and static SEMIEA high pressure which causes the isobars to close up and sometimes, depending on the latitude of the low-pressure system, create the narrow SW to NE atmospheric river.

1.19 *The WAP Increases the Temperature in Northern Europe*

The LME and MERRA-2 data in Table 1 (F)(1-2) show statistically significant connections between the WAP AOD and TS in Europe. All datasets at (F)(3-5) and Figure 11 show increasing TS as the WAP AOD level increases and note that in Table 1 (F)(3) the MERRA-2 and Terra-NCEP/NCAR data shows a larger increase than the LME per unit WAP AOD. Figure A15 shows an increase of over 4º K across much of Europe north of the Alps.

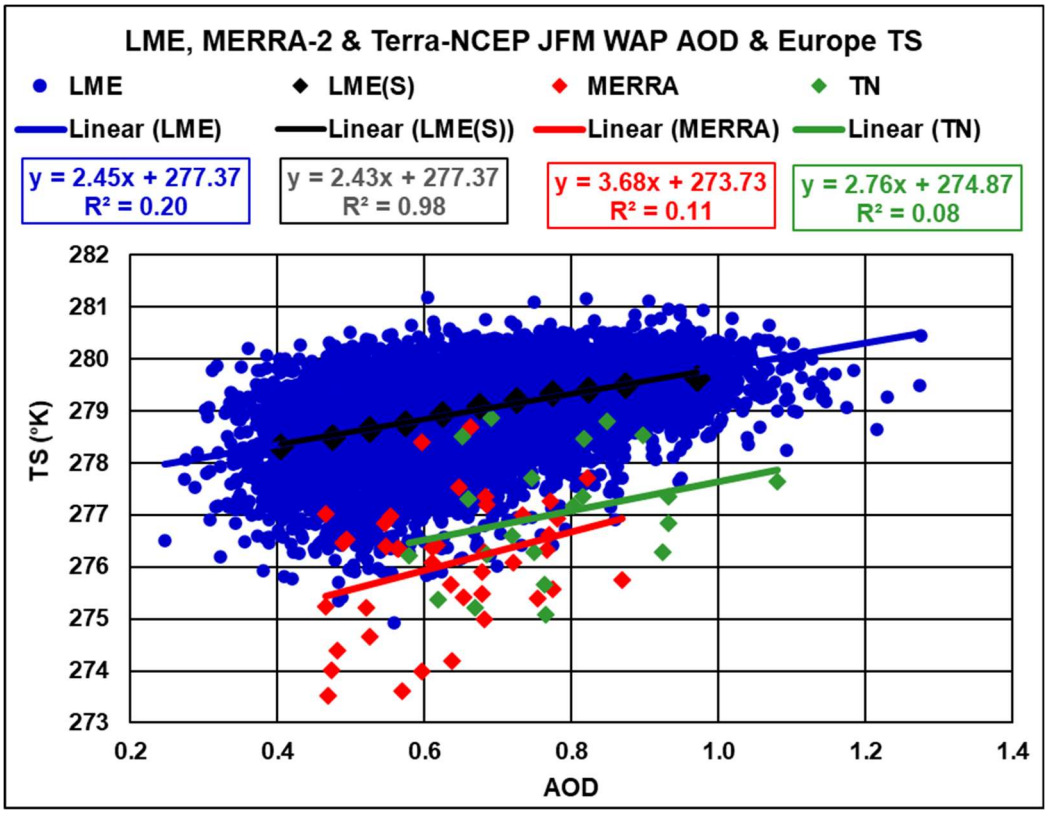

Figure 11. LME, MERRA-2 and Terra-NCEP/NCAR JFM Northern European Temperature and WAP Area AOD.

DISCUSSION

Correlation between events A and B does not prove causation from A to B or vice versa. The causal relationship between the WAP and the European climate is demonstrated here.

1.20 *Multiple Datasets*

Preprints (www.preprints.org) | NOT PEER-REVIEWED | Posted: 31 August 2021 doi:10.20944/preprints202108.0554.v1

Three independent datasets: the LME, with 1,156 years of data and eight different forcing scenarios; the MERRA-2 reanalysis with 41 years of data including assimilated aerosol measurements; and Terra-NCEP/NCAR with 21 years of measured aerosol data all show the same trends in the parameters analysed and 20 out of 24 analyses show statistically significant connections.

1.21 Analysis without Correlation

The results reflect actual measurements.

1.21.1 Pressure over the SEMIEA

When the LME PSL data from all simulations/runs in years when WAP AOD is below 0.45 and above 0.90 is averaged the PSL change from low AOD to high is 7.2 hPa which mirrors the reported trend [11] whereas the modelling in that paper does not. The Terra-NCEP/NCAR data shows an even higher positive trend in PSL than the LME whilst MERRA-2 shows a lower but still significant positive trend.

1.21.2 Precipitation in Iberia

When the LME PRECL data from all simulations/runs in years when WAP AOD is below 0.45 and above 0.90 is averaged the reduction from low AOD to high is 103mm (59%) which nearly exactly matches the 60% measured Iberian rainfall reduction [6]. The average of all four datasets in Table 1(D)(6) shows a similar reduction from the WAP AOD in 1950 to the high at 75%.

1.21.3 Precipitation in The U.K.

When the LME PRECL data from all simulations/runs in years when WAP AOD is below 0.45 and above 0.90 is averaged the change from low AOD to high is 127mm or 28% which is the same order of magnitude as the change in the recorded UK (ex Northern Ireland) rainfall (UK Met Office at https://www.metoffice.gov.uk/research/climate/maps-and-data/uk-and-regional-series) from the average from 1862 to 1988 to the average from 1989 to 2020 at 17%.

1.21.4 Warmer Temperatures in Europe.

Using the trend in the "all simulation" LME TS data, 2.45º K per unit AOD increase, the TS change from the estimated low AOD of 0.09 in 1950 to the measured high in the Terra FM AOD data in Figure 2, 1.2 (2000), is 2.72º K which mirrors the reported trend [11] and the CRUTEM.4.6.0.0 land temperature data [32] trend of +2.90º K from 1950 to 2007.

1.21.5 Modelling

LME: there is no physical mechanism by which drought or SLP in SEMIEA can create aerosols in the LME over West Africa hence the causal direction must run from the aerosols to the PSL, PRECL and TS and the aerosol forcings in all LME runs are fixed at 1850 values except for the "ozone and aerosol" and "all" runs and there can therefore be no forcing of the aerosols by any agent within these six runs and the causal direction must flow from the aerosols.

Preprints (www.preprints.org) | NOT PEER-REVIEWED | Posted: 31 August 2021 doi:10.20944/preprints202108.0554.v1

MERRA-2: assimilates measured aerosol data and therefore the causal direction must be from the aerosols to the rainfall and SLP as it cannot be the reverse.

Terra-NCEP/NCAR: this dataset includes measured aerosol data and, as stated in Appendix B, the source of the WAP aerosols is undoubtably fires and gas flares in West Africa.

1.21.6 Multiple Independent Datasets in the LME

The eight LME modelling runs exhibit very low or negative correlations between the WAP AOD in the individual runs as shown in the correlation matrix in Appendix F with an overall average 0.0016. Hence the datasets are independent.

All eight LME datasets show correlations at magnitude -0.62 and 0.74 or greater with the Iberian rainfall and SEMIEA SLP respectively at significance of <0.01 or less and the chance that all these eight independent datasets show the same result and are wrong is the product of the significance i.e., 0.01^8 or 10^{-17}, a vanishingly small number.

1.21.7 Another Event "C"

One possible explanation for the correlations shown in this paper is that an unknown event "C" causes the WAP all the other effects discussed in this paper simultaneously.

Appendix B shows the JFM WAP is unquestionably anthropogenic caused by biomass burning in deliberately lit fires in West Africa and gas flares and it is therefore impossible for another event to cause the WAP and the changes in Europe discussed here and this possibility must be rejected.

Preprints (www.preprints.org) | NOT PEER-REVIEWED | Posted: 31 August 2021 doi:10.20944/preprints202108.0554.v1

1.22 CAUSAL DIRECTION

Therefore with:

1. All the datasets showing as the WAP Area AOD rises:
   a. Increasing SEMEIEA pressure;
   b. Increasing UK rainfall;
   c. Reducing Iberian rainfall;
   d. Increasing northern European temperatures.
2. The LME analysis showing the same results across multiple independent datasets with a vanishingly small chance of error;

the inevitable conclusion is that the WAP is the primary driver in JFM of increased pressure over the SEMIEA, and a significant driver of increased rainfall in the UK, increased temperatures in northern Europe and reduced rainfall in Iberia.

1.23 FUTURE RESEARCH

1.23.1 Confirming the conclusions

An LME style analysis should be undertaken in which a WAP ramps up from the November 1950 AOD level to reach the same January AOD as the extreme 2004 JFM WAP, continues at the same level to March and ramps down in April to the May 1950 level. This plume to be applied with random returns from 3 to 10 years with all other forcing agents held constant.

This modelling should be repeated with AOD levels reduced by 10% between runs to determine the level of AOD in the WAP Area which is required to perturb the European climate.

This will provide the information governments require to reduce the WAP AOD to levels which will not impact the winter climate of Europe.

1.24 Mitigating the WAP

1.24.1 Seasonal Biomass Burning

Biomass burning is the most significant source of JFM aerosols and occurs for the reasons outlined in Appendix B.

New technologies could reduce biomass burning by converting the biomass into useful products such as liquid fuel [33] [34] and may quickly reduce the WAP AOD levels as the technology would create a new income stream for those selling into a new industry and West African governments could then ban biomass burning in the open.

1.24.2 Gas Flares

The WAP also comprises carbonaceous aerosols from oil industry flaring of associated gas (Appendix B). The World Bank Global Gas Flaring Reduction Partnership (GGFRP) has been working to reduce routine flaring and reports Nigeria reduced flaring from 8.4 to 7.4 billion cubic metres between 2014 and 2018 (https://www.worldbank.org/en/programs/gasflaringreduction#7)

However, Nigeria was the 7th largest flaring country in the World in 2018 (GGFRP) and the industry should be required to immediately eliminate the routine flaring of gas which creates aerosols.

1.24.3 Background AOD Levels

Preprints (www.preprints.org) | NOT PEER-REVIEWED | Posted: 31 August 2021 doi:10.20944/preprints202108.0554.v1

Background AOD levels is the average April to November level when the monsoon prevents biomass burning.

The representative concentration pathway data from the International Institute for Applied Systems Analysis (IIASA) at https://www.iiasa.ac.at/web/home/research/researchPrograms/TransitionstoNewTechnologies/RCP.en.html shows no change in carbonaceous aerosols from the Middle East and Africa before 1950 and then a sixfold increase by 2000 with the majority of the increase occurring by 1970. Hence as West Africa is one of the regions where there has been a significant increase it is obvious that the WAP Area background AOD level in 1950 must have been significantly lower than the 0.41 level shown in Figure 2. It is therefore possible that this increased background level since 1950 may have also affected the European climate in other seasons and this requires further research.

1.24.4 Other Aerosol Plumes

Eight continental scale aerosol plumes now exist in the World each year, each in its own season [14]. Research on the apparitions of these plumes must focus on their seasonal effects on inter alia: the climate of Europe in summer and autumn; Australian and Sahelian drought; Arctic Ice levels; and ENSO.

CONCLUSIONS

The LME (1.156 years of data), MERRA-2 (41 years) and Terra-NCEP/NCAR (21 years) confirm the direct connection between the WAP and the European winter climate in multiple independent ways and analysis clearly shows that the relationship must be causal.

I therefore conclude:

1. The WAP is the prime trigger for and sustaining influence on changes in the winter climate of Europe driving increased pressure over SEMIEA which then creates increased UK rainfall, Iberian drought and increased northern European temperatures.
2. The climate modelling cited in the introduction failed to replicate the significant observed surface pressure rise over the Mediterranean as the models did not accurately incorporate the carbonaceous, anthropogenic aerosols of the WAP.
3. The WAP and the other seven continental scale aerosol plumes which now exist each year must be incorporated in climate analysis at spatial and temporal resolutions that do not lose the effects of the plumes due to averaging. A spatial resolution of less than 2° of latitude and longitude and a temporal resolution of less than 1 month should suffice.
4. As the WAP changes the climate of Europe it is obviously possible that the other seven continental scale aerosol plumes may have effects which are even more remote from the plume than the WAP is from Europe and this requires investigation.

Finally I concur with [35] that emissions of carbonaceous aerosols are directly addressable by government policy and suggest that this is an urgent necessity to restore the winter climate of Europe to its pre-WAP, natural state circa 1950.

Preprints (www.preprints.org) | NOT PEER-REVIEWED | Posted: 31 August 2021 doi:10.20944/preprints202108.0554.v1

SUPPLEMENTARY INFORMATION

Appendix A The eight continental scale aerosol plumes
Appendix B Sources of The West African Aerosol Plume
Appendix C Aerosols and Climate
Appendix D Data Sources
Appendix E Comparison of the Effects of the 2004 and 1987 WAP
Appendix F Correlation Matrix for LME and MERRA-2 AOD

FUNDING

This research project was funded entirely by the author and his wife, Julie and received no external funding.

DATA AVAILABILITY

Data sources which are all publicly available are listed in Appendix D.0

Preprints (www.preprints.org) | NOT PEER-REVIEWED | Posted: 31 August 2021 doi:10.20944/preprints202108.0554.v1

CONFLICTS OF INTEREST

The author declares no conflict of interest.

ACKNOWLEDGEMENTS

I acknowledge:

NASA: Analyses and visualizations used in this paper were produced with the Giovanni online data system, developed and maintained by the NASA GES DISC; the mission scientists and Principal Investigators who provided the data and images used in this paper including the MERRA-2 data; and Dr Robert Schmunk for the Panoply data viewer;

NASA for the fire data at https://earthdata.nasa.gov/earth-observation-data/near-real-time/firms/active-fire-data ;

NASA for the CALIPSO data obtained from the NASA Langley Research Center Atmospheric Science Data Center at https://eosweb.larc.nasa.gov/project/calipso/calipso_table .

The NOAA/ESRL Physical Sciences Division, Boulder Colorado for the data and images from their Web site at http://www.esrl.noaa.gov/psd/ .

The CESM1(CAM5) Last Millennium Ensemble Community Project and supercomputing resources provided by NSF/CISL/Yellowstone;

The UK Met Office at https://www.metoffice.gov.uk/weather/learn-about/past-uk-weather-events for the UK flood information, rainfall and temperature data;

The IPCC for the images and Assessment Reports;

Google Earth™ and the copyright holders noted on the image for the image of the Earth;

The United Nations Department of Economic and Social Affairs Population Division for the world population statistics at https://www.un.org/en/development/desa/population/publications/database/index.asp;

BP for the oil production statistics at https://www.bp.com/en/global/corporate/energy-economics/statistical-review-of-world-energy.html

The Global Gas Flaring Reduction Partnership (World Bank and NOAA) for the gas flare data and image at https://www.worldbank.org/en/programs/gasflaringreduction ;

The Global Volcanism Program at the Smithsonian Institution for the volcano eruption data. http://dx.doi.org/10.5479/si.GVP.VOTW4-2013 ;

Global Forest Watch for the forest data https://www.globalforestwatch.org/

Preprints (www.preprints.org) | NOT PEER-REVIEWED | Posted: 31 August 2021 doi:10.20944/preprints202108.0554.v1

References

1. Chiverrell, R.C.; Sear, D.A.; Warburton, J.; Macdonald, N.; Schillereff, D.N.; Dearing, J.A.; Croudace, I.W.; Brown, J.; Bradley, J. Using lake sediment archives to improve understanding of flood magnitude and frequency: Recent extreme flooding in northwest UK. *Earth Surface Processes and Landforms* **2019**, *44*, 2366-2376, doi:10.1002/esp.4650.
2. Gelaro, R.; McCarty, W.; Suárez, M.J.; Todling, R.; Molod, A.; Takacs, L.; Randles, C.A.; Darmenov, A.; Bosilovich, M.G.; Reichle, R.; et al. The Modern-Era Retrospective Analysis for Research and Applications, Version 2 (MERRA-2). *Journal of Climate* **2017**, *30*, 5419-5454, doi:10.1175/jcli-d-16-0758.1.
3. Huntingford, C.; Marsh, T.; Scaife, A.A.; Kendon, E.J.; Hannaford, J.; Kay, A.L.; Lockwood, M.; Prudhomme, C.; Reynard, N.S.; Parry, S.; et al. Potential influences on the United Kingdom's floods of winter 2013/14. *Nature Clim. Change* **2014**, *4*, 769-777, doi:10.1038/nclimate2314.
4. Schaller, N.; Kay, A.L.; Lamb, R.; Massey, N.R.; van Oldenborgh, G.J.; Otto, F.E.L.; Sparrow, S.N.; Vautard, R.; Yiou, P.; Ashpole, I.; et al. Human influence on climate in the 2014 southern England winter floods and their impacts. *Nature Clim. Change* **2016**, *6*, 627-634, doi:10.1038/nclimate2927

http://www.nature.com/nclimate/journal/v6/n6/abs/nclimate2927.html#supplementary-information.
5. Lavers, D.A.; Allan, R.P.; Wood, E.F.; Villarini, G.; Brayshaw, D.J.; Wade, A.J. Winter floods in Britain are connected to atmospheric rivers. *Geophysical Research Letters* **2011**, *38*, doi:10.1029/2011gl049783.
6. García-Herrera, R.; Paredes, D.; Trigo, R.M.; Trigo, I.F.; Hernández, E.; Barriopedro, D.; Mendes, M.A. The Outstanding 2004/05 Drought in the Iberian Peninsula: Associated Atmospheric Circulation. *Journal of Hydrometeorology* **2007**, *8*, 483-498, doi:10.1175/jhm578.1.
7. Vicente-Serrano, S.M.; López-Moreno, J.I. The influence of atmospheric circulation at different spatial scales on winter drought variability through a semi-arid climatic gradient in Northeast Spain. *International Journal of Climatology* **2006**, *26*, 1427-1453, doi:10.1002/joc.1387.
8. Yiou, P.; Vautard, R.; Naveau, P.; Cassou, C. Inconsistency between atmospheric dynamics and temperatures during the exceptional 2006/2007 fall/winter and recent warming in Europe. *Geophysical Research Letters* **2007**, *34*, doi:10.1029/2007gl031981.
9. Cattiaux, J.; Vautard, R.; Cassou, C.; Yiou, P.; Masson-Delmotte, V.; Codron, F. Winter 2010 in Europe: A cold extreme in a warming climate. *Geophysical Research Letters* **2010**, *37*, doi:10.1029/2010gl044613.
10. Luterbacher, J.; Liniger, M.A.; Menzel, A.; Estrella, N.; Della-Marta, P.M.; Pfister, C.; Rutishauser, T.; Xoplaki, E. Exceptional European warmth of autumn 2006 and winter 2007: Historical context, the underlying dynamics, and its phenological impacts. *Geophysical Research Letters* **2007**, *34*, doi:10.1029/2007gl029951.
11. van Oldenborgh, G.J.; Drijfhout, S.; van Ulden, A.; Haarsma1, R.; Sterl, A.; Severijns, C.; Hazeleger, W.; Dijkstra, H. Western Europe is warming much faster than expected. *Climate of the Past* **2009**, *5*, 1 - 12.
12. Osborn, T.J. Simulating the winter North Atlantic Oscillation: the roles of internal variability and greenhouse gas forcing. *Climate Dynamics* **2004**, *22*, doi:10.1007/s00382-004-0405-1.
13. Sterl, A.; Severijns, C.; Dijkstra, H.; Hazeleger, W.; Jan van Oldenborgh, G.; van den Broeke, M.; Burgers, G.; van den Hurk, B.; Jan van Leeuwen, P.; van Velthoven, P. When can we

Preprints (www.preprints.org) | NOT PEER-REVIEWED | Posted: 31 August 2021 doi:10.20944/preprints202108.0554.v1

expect extremely high surface temperatures? *Geophysical Research Letters* **2008**, *35*, doi:10.1029/2008gl034071.

14. Potts, K.A. Poster: How the Natural & Anthropogenic Aerosol Plume over S. E. Asia caused the Millennium Drought. In Proceedings of the AMOS-ICSHMO 2018, Sydney, Australia, 2018.
15. Kaufman, Y.J.; Holben, B.N.; Tanré, D.; Slutsker, I.; Smirnov, A.; Eck, T.F. Will aerosol measurements from Terra and Aqua Polar Orbiting satellites represent the daily aerosol abundance and properties? *Geophysical Research Letters* **2000**, *27*, 3861-3864, doi:10.1029/2000GL011968.
16. Remer, L.A.; Kaufman, Y.J.; Tanré, D.; Mattoo, S.; Chu, D.A.; Martins, J.V.; Li, R.R.; Ichoku, C.; Levy, R.C.; Kleidman, R.G.; et al. The MODIS Aerosol Algorithm, Products, and Validation. *Journal of the Atmospheric Sciences* **2005**, *62*, 947-973, doi:10.1175/JAS3385.1.
17. Remer, L.; RC, L.; S, M.; D, T.; P, G.; Y, S.; V, S.; LA, M.; Y, Z.; M, K.; et al. The Dark Target Algorithm for Observing the Global Aerosol System: Past, Present, and Future. *Remote Sensing of Environment* **2020**, *12*, doi:10.3390/rs12182900.
18. Oluleye, A.; Ogunjobi, K.O.; Bernard, A.; Ajayi, V.O.; A.A., A. Multiyear Analysis of Ground-Based Sunphotometer (AERONET) Aerosol Optical Properties and its Comparison with Satellite Observations over West Africa. *Global Journal of HUMAN SOCIAL SCIENCE Geography & Environmental GeoSciences* **2012**, *12*.
19. Ramanathan, V. ATMOSPHERIC BROWN CLOUDS: HEALTH, CLIMATE AND AGRICULTURE IMPACTS. *Scripta Varia* **2006**, *106*.
20. Duncan, B.N.; Bey, I.; Chin, M.; Mickley, L.J.; Fairlie, T.D.; Martin, R.V.; Matsueda, H. Indonesian wildfires of 1997: Impact on tropospheric chemistry. *Journal of Geophysical Research: Atmospheres* **2003**, *108*, 4458, doi:10.1029/2002JD003195.
21. Hansell, R.A.; Tsay, S.C.; Ji, Q.; Liou, K.N.; Ou, S.C. Surface aerosol radiative forcing derived from collocated ground-based radiometric observations during PRIDE, SAFARI, and ACE-Asia. *Appl Opt* **2003**, *42*, 5533-5544.
22. Hammer, Ø.; Harper, D.A.T.; Ryan, P.D. PAST: Paleontological statistics software package for education and data analysis. . *Palaeontologia Electronica 4(1): 9pp* **2001**, 9pp.
23. Otto-Bliesner, B.L.; Brady, E.C.; Fasullo, J.; Jahn, A.; Landrum, L.; Stevenson, S.; Rosenbloom, N.; Mai, A.; Strand, G. Climate Variability and Change since 850 CE: An Ensemble Approach with the Community Earth System Model. *Bulletin of the American Meteorological Society* **2016**, *97*, 735-754, doi:10.1175/bams-d-14-00233.1.
24. Kalnay, E.; Kanamitsu, M.; Kistler, R.; Collins, W.; Deaven, D.; Gandin, L.; Iredell, M.; Saha, S.; White, G.; Woollen, J.; et al. The NCEP/NCAR 40-Year Reanalysis Project. *Bulletin of the American Meteorological Society* **1996**, *77*, 437-471, doi:10.1175/1520-0477(1996)077<0437:TNYRP>2.0.CO;2.
25. Winker, D.M.; Vaughan, M.A.; Omar, A.; Hu, Y.; Powell, K.A.; Liu, Z.; Hunt, W.H.; Young, S.A. Overview of the CALIPSO Mission and CALIOP Data Processing Algorithms. *Journal of Atmospheric and Oceanic Technology* **2009**, *26*, 2310-2323, doi:10.1175/2009jtecha1281.1.
26. McGregor, G.R.; Nieuwolf, S. *Tropical Climatology*; John Wiley and Sons: 1977; p. 207.
27. Barry, R.G.; Chorley, R.J. *Atmosphere Weather and Climate* Routledge, Abingdon UK: 2010.
28. IPCC. IPCC Assessment Report 4 Glossary. **2007**.
29. Ralph, F.M.; Dettinger, M.D. Storms, floods, and the science of atmospheric rivers. *Eos, Transactions American Geophysical Union* **2011**, *92*, 265-266, doi:10.1029/2011eo320001.
30. Lavers, D.A.; Villarini, G. The nexus between atmospheric rivers and extreme precipitation across Europe. *Geophysical Research Letters* **2013**, *40*, 3259-3264, doi:10.1002/grl.50636.

Preprints (www.preprints.org) | NOT PEER-REVIEWED | Posted: 31 August 2021 doi:10.20944/preprints202108.0554.v1

31. Young, A.M.; Skelly, K.T.; Cordeira, J.M. High-impact hydrologic events and atmospheric rivers in California: An investigation using the NCEI Storm Events Database. *Geophysical Research Letters* **2017**, *44*, 3393-3401, doi:10.1002/2017GL073077.
32. Jones, P.D.; Lister, D.H.; Osborn, T.J.; Harpham, C.; Salmon, M.; Morice, C.P. Hemispheric and large-scale land-surface air temperature variations: An extensive revision and an update to 2010. *Journal of Geophysical Research: Atmospheres* **2012**, *117*, doi:10.1029/2011jd017139.
33. Seifkar, N.; Lu, X.; Withers, M.; Malina, R.; Field, R.; Barrett, S.; Herzog, H. *Biomass to Liquid Fuels Pathways*; 2015.
34. Graham, P.W.; Brinsmead, T.S.; Reedman2, L.J. *An assessment of competition for biomass resources within the energy and transport sectors*; CSIRO: 2011.
35. Booth, B.B.; Dunstone, N.J.; Halloran, P.R.; Andrews, T.; Bellouin, N. Aerosols implicated as a prime driver of twentieth-century North Atlantic climate variability. *Nature* **2012**, *484*, 228-232, doi:10.1038/nature10946.